

Real-space renormalization study of a quantum spin glass with Ruderman-Kittel-Kasuya-Yosida interactions

U. Sannemo and K. A. Chao

Department of Physics and Measurement Technology, University of Linköping, S-58183 Linköping, Sweden

(Received 13 November 1986)

We have performed a real-space renormalization calculation to investigate the low-temperature properties of 54 randomly located quantum spins ($s = \frac{1}{2}$) with Ruderman-Kittel-Kasuya-Yosida interactions. The computed spin-glass order parameter, dc magnetic susceptibility, magnetic specific heat, internal field distribution, and spatial correlation of eigenstates suggest a progressive freezing of spins with decreasing temperature.

I. INTRODUCTION

The random nature of the exchange interaction in a spin glass does not allow the system to exhibit long-range magnetic order, but at low temperature freezes the spins in random directions. Although experimental observations on physical properties around the magnetic susceptibility cusp have provided information in favor of a sharp phase transition over a progressive freezing of the spins, whether a thermodynamic phase transition between paramagnetic and spin-glass phases exists in three dimensions remains the central issue of spin-glass theory. Recently, there have been several reviews on the present understanding of spin glasses.¹

Theories have been developed extensively mainly for spin glasses in either an Ising or Heisenberg system of classical spins. For infinite-range interaction the Sherrington-Kirkpatrick² model exhibits a thermodynamic phase transition. On the other hand, for short-range interaction in three dimensions, numerical studies suggest a finite transition temperature in the Ising model,³ but zero transition temperature in the Heisenberg model.⁴ For a more realistic investigation of metallic spin glasses, it is necessary to consider quantum spin systems with Ruderman-Kittel-Kasuya-Yosida (RKKY) interaction.

Almost all existing theoretical works on quantum spin glasses are within the framework of the mean-field approximation. For the Edwards-Anderson model,⁵ Fischer⁶ found a cusp in the susceptibility and in the specific heat. A conflicting result was obtained by Klemm⁷ who speculated that the quantum fluctuations may destroy the spin-glass transition for spin $\frac{1}{2}$. Bray and Moore⁸ have reexamined the same problem and discovered that the quantum fluctuations depress the transition but do not destroy it. Using a generalized Thouless-Anderson-Palmer equation,⁹ Sommers and Usadel¹⁰ detected a spin-glass state in two-level systems. The effect of quantum fluctuations in the Edwards-Anderson model with anisotropic exchange was also analyzed recently by Morris¹¹ and Theumann.¹² Nishimori *et al.*¹³ have performed numerical calculations to study the spin- $\frac{1}{2}$ random Heisenberg model with infinite-range interaction in a finite cluster of maximum 16 spins. They found a critical point

between the spin-glass and the mixed-ferromagnetic phases.

Theoretical analysis of quantum spin glasses with RKKY interaction is very difficult. Most existing results have been derived numerically with a system of randomly distributed classical Heisenberg spins. The works of Ching and Huber¹⁴ and Fernandez and Streit¹⁵ are not very conclusive. Walstedt and Walker,¹⁶ Walstedt,¹⁷ and Walker and Walstedt¹⁸ found no spin-glass state with pure RKKY interaction, whereas with a small amount of anisotropy the system exhibits evidence for spin freezing at low temperature. Their Monte Carlo calculations have been improved by Chakrabarti and Dasgupta¹⁹ with a correction for any uniform rotation of the spin system. The finite-size-scaling result of Chakrabarti and Dasgupta indicates a zero-temperature critical point for the spin-glass phase. The recent analysis of Bray *et al.*²⁰ suggests that in a classical Heisenberg spin system with RKKY interaction, the dependence of the glass transition temperature T_f on anisotropy D is logarithmic, and $T_f \rightarrow 0$ as $D \rightarrow 0$.

In this paper we will perform a numerical renormalization study on quantum Heisenberg spin glass with RKKY interaction. The renormalization scheme is presented in Sec. II, and then applied to a finite cluster of random spins in Sec. III. In Sec. IV the characteristic features of the eigenstates will be analyzed together with the spatial distribution of internal magnetic fields. The low-temperature spin-glass behavior of the system will be demonstrated in Sec. V, which contains the computed Edwards-Anderson order parameter, the magnetic susceptibility, and the magnetic specific heat.

II. RENORMALIZATION SCHEME

In this section we will outline the mathematical structure of the renormalization procedure for our calculation. The scheme is based on the truncation method originally introduced in the study of lattice-field theory.²¹ The method has been used by many authors to study Kondo-lattice,²² Ising and XY models in transverse field,²³ quantum-lattice systems,^{24,25} the Hubbard model,²⁶ and one-dimensional magnetic systems.²⁷⁻²⁹

We consider a spin- $\frac{1}{2}$ Heisenberg Hamiltonian in a uniform external magnetic field $\mathbf{B}=B(0,0,1)$,

$$H = \sum_{i,j=1}^N \mathcal{J}_{0:ij} \mathbf{S}_i \cdot \mathbf{S}_j + \sum_{i=1}^N \mathbf{B} \cdot \mathbf{S}_i . \quad (1)$$

The positions of spins are random, and $\mathcal{J}_{0:ij}$ can be any kind of exchange interaction with $\mathcal{J}_{0:ii}=0$. The system of N spins is divided into $M(0)$ blocks, and each block contains $N(0)=N/M(0)$ spins. Let $I_0=1, 2, \dots, M(0)$ label the blocks. The spins in the I_0 th block are specified as $\mathbf{S}_{I_0,i}$ with $i=1, 2, \dots, N(0)$, and the exchange interaction between $\mathbf{S}_{I_0,i}$ and $\mathbf{S}_{J_0,j}$ is reexpressed as $\mathcal{J}_{I_0,i;J_0,j}$. Then (1) can be written as

$$H = \sum_{I_0=1}^{M(0)} H(0:I_0) + \sum_{I_0, J_0=1}^{M(0)} H(0:I_0, J_0)(1 - \delta_{I_0, J_0}) , \quad (2)$$

where

$$H(0:I_0) = \sum_{i,j \in I_0} \mathcal{J}_{I_0,i;I_0,j} \mathbf{S}_{I_0,i} \cdot \mathbf{S}_{I_0,j} + \sum_{i \in I_0} \mathbf{B} \cdot \mathbf{S}_{I_0,i} , \quad (3)$$

and

$$H(0:I_0, J_0) = \sum_{i \in I_0} \sum_{j \in J_0} \mathcal{J}_{I_0,i;J_0,j} \mathbf{S}_{I_0,i} \cdot \mathbf{S}_{J_0,j} . \quad (4)$$

Let $\{|\Phi(0:I_0)_i\rangle; i=1, 2, \dots, \mu(0)\}$ be the set of configurations of the spins in the I_0 th block, where $\mu(0)=2^{N(0)}$. $H(0:I_0)$ and $H(0:I_0, J_0)$ will be expressed in more convenient forms

$$H(0:I_0) = \sum_{i,j \in I_0} |\Phi(0:I_0)_i\rangle H(0:I_0)_{ij} \langle \Phi(0:I_0)_j| \quad (5)$$

and

$$H(0:I_0, J_0) = \sum_{i,k \in I_0} \sum_{j,l \in J_0} |\Phi(0:I_0)_i\rangle |\Phi(0:J_0)_j\rangle \times H(0:I_0, J_0)_{jilk} \times \langle \Phi(0:I_0)_k| \langle \Phi(0:J_0)_l| , \quad (6)$$

where

$$H(0:I_0)_{ij} = \langle \Phi(0:I_0)_i | H(0:I_0) | \Phi(0:I_0)_j \rangle \quad (7)$$

and

$$H(0:I_0, J_0)_{jilk} = \langle \Phi(0:J_0)_j | \langle \Phi(0:I_0)_i | H(0:I_0, J_0) \times |\Phi(0:J_0)_l\rangle |\Phi(0:I_0)_k\rangle . \quad (8)$$

For given value of $N(0)$, the Schrödinger equation

$$H(0:I_0) |\Psi(1:I_0)_i\rangle = E(1:I_0)_i |\Psi(1:I_0)_i\rangle \quad (9)$$

is solved exactly with eigenstates

$$|\Psi(1:I_0)_i\rangle = \sum_{\alpha=1}^{\mu(0)} U(0:I_0)_{i\alpha} |\Phi(0:I_0)_\alpha\rangle . \quad (10)$$

Because the external magnetic field lifts all spin degeneracies, the eigenenergies can be ordered as $E(0:I_0)_i < E(0:I_0)_j$ if $i < j$.

In terms of the basis $\{|\Psi(1:I_0)_i\rangle; i=1, 2, \dots, \mu(0)\}$, we can write (5) and (6) in the forms

$$H(0:I_0) = \sum_{i,j \in I_0} |\Psi(1:I_0)_i\rangle \tilde{H}(0:I_0)_{ij} \langle \Psi(1:I_0)_j| \quad (11)$$

and

$$H(0:I_0, J_0) = \sum_{i,k \in I_0} \sum_{j,l \in J_0} |\Psi(1:I_0)_i\rangle |\Psi(1:J_0)_j\rangle \times \tilde{H}(0:I_0, J_0)_{jilk} \times \langle \Psi(1:I_0)_k| \langle \Psi(1:J_0)_l| , \quad (12)$$

where

$$\tilde{H}(0:I_0)_{ij} = E(1:I_0)_i \delta_{ij} \quad (13)$$

and

$$\tilde{H}(0:I_0, J_0)_{jilk} = \sum_{\alpha, \beta, \gamma, \lambda=1}^{\mu(0)} U(0:I_0)_{\alpha i}^\dagger U(0:J_0)_{\beta j}^\dagger \times U(0:I_0)_{k\gamma} U(0:J_0)_{l\lambda} \times H(0:I_0, J_0)_{\beta\alpha\lambda\gamma} . \quad (14)$$

We are interested in the low-temperature properties of the system, which are dominated by the low-lying eigenstates. Therefore, for each I_0 we will truncate the energy spectrum $E(1:I_0)_i$ and keep only the ξ lowest eigenenergies $i=1, 2, \dots, \xi$. Next, we combine every set of η blocks into a new block according to the rule that the first η old blocks $I_0=1, 2, \dots, \eta$ become the first new block, the second η old blocks $I_0=\eta+1, \eta+2, \dots, 2\eta$ become the second new block, and so on. Let the new blocks be labeled by $I_1=1, 2, \dots, M(1)$, where $M(1)=M(0)/\eta$. So the η old blocks specified by $I_0=(I_1-1)\eta+1, (I_1-1)\eta+2, \dots, I_1\eta$ belong to the I_1 th new block. Now, we redefine the summations in (11) and (12) as restricted sums which run over only the ξ lowest eigenstates $\{|\Psi(1:I_0)_i\rangle; i=1, 2, \dots, \xi\}$. Then, from (2), (11), and (12) we can construct the truncated Hamiltonian as

$$H \simeq \sum_{I_1=1}^{M(1)} H(1:I_1) + \sum_{I_1, J_1=1}^{M(1)} H(1:I_1, J_1)(1 - \delta_{I_1, J_1}) , \quad (15)$$

where

$$H(1:I_1) = \sum_{I_0, J_0 \in I_1} H(0:I_0, J_0)(1 - \delta_{I_0, J_0}) + \sum_{I_0 \in I_1} H(0:I_0) \quad (16)$$

and

$$H(1:I_1, J_1) = \sum_{I_0 \in I_1} \sum_{J_0 \in J_1} H(0:I_0, J_0) . \quad (17)$$

We define the configurations in the I_1 th block as

$$|\phi(1:I_1)_{p_1 p_2 \dots p_\eta}\rangle = \prod_{i=1}^{\eta} |\psi(1:I_{0,i})_{p_i}\rangle , \quad p_i = 1, 2, \dots, \xi , \quad (18)$$

where $I_{0,i}$ is one of the I_0 's which belong to I_1 . Altogether, there are $\mu(1)=\xi^\eta$ such configurations. For convenience, we can use any suitable rule to order these configurations. With a new notation, we write the ordered configurations as $|\phi(1:I_1)_i\rangle$, where $i=1, 2, \dots, \mu(1)$. In terms of these configurations, (16) and (17) are then expressed in the forms

$$H(1:I_1) = \sum_{i,j \in I_1} |\Phi(1:I_1)_i\rangle H(1:I_1)_{ij} \langle \Phi(1:I_1)_j| \quad (19)$$

and

$$H(1:I_1, J_1) = \sum_{i,k \in I_1} \sum_{j,l \in J_1} |\Phi(1:I_1)_i\rangle |\Phi(1:J_1)_j\rangle \times H(1:I_1, J_1)_{jilk} \times \langle \Phi(1:I_1)_k | \langle \Phi(1:J_1)_l |, \quad (20)$$

where

$$H(1:I_1)_{ij} = \langle \Phi(1:I_1)_i | H(1:I_1) | \Phi(1:I_1)_j \rangle \quad (21)$$

and

$$H(1:I_1, J_1)_{jilk} = \langle \Phi(1:J_1)_j | \langle \Phi(1:I_1)_i | H(1:I_1, J_1) \times | \Phi(1:J_1)_l | | \Phi(1:I_1)_k \rangle. \quad (22)$$

The single-block Hamiltonian (19) is again diagonalized to yield $\mu(1)$ eigenenergies $E(2:I_1)_i$ and the associated eigenstates

$$|\Psi(2:I_1)_i\rangle = \sum_{\alpha=1}^{\mu(1)} U(1:I_1)_{i\alpha} |\Phi(1:I_1)_\alpha\rangle. \quad (23)$$

Using the transformation matrix $\underline{U}(1:I_1)$, (19) and (20) are transformed to

$$H(1:I_1) = \sum_{i,j \in I_1} |\Psi(2:I_1)_i\rangle \tilde{H}(1:I_1)_{ij} \langle \Psi(2:I_1)_j| \quad (24)$$

and

$$H(1:I_1, J_1) = \sum_{i,k \in I_1} \sum_{j,l \in J_1} |\Psi(2:I_1)_i\rangle |\Psi(2:J_1)_j\rangle \times \tilde{H}(1:I_1, J_1)_{jilk} \times \langle \Psi(2:I_1)_k | \langle \Psi(2:J_1)_l |, \quad (25)$$

where

$$\tilde{H}(1:I_1)_{ij} = E(2:I_1)_i \delta_{ij} \quad (26)$$

and

$$\tilde{H}(1:I_1, J_1)_{jilk} = \sum_{\alpha,\beta,\gamma,\lambda=1}^{\mu(1)} U(1:I_1)_{i\alpha}^\dagger U(1:J_1)_{\beta j}^\dagger \times U(1:I_1)_{k\gamma} U(1:J_1)_{l\lambda} \times H(1:I_1, J_1)_{\beta\alpha\lambda\gamma}. \quad (27)$$

Equations (15) and (24)–(27) have exactly the same structures as Eqs. (2) and (11)–(14). Therefore, we can repeat the renormalization operation until the fixed point is reached.

After ν renormalizations if within a given accuracy the matrix $\underline{H}(v:I_\nu)$ becomes diagonal and the matrices $\underline{H}(v:I_\nu, J_\nu)$ reduce to zero for all I_ν and J_ν , then the renormalization procedure reaches the fixed-point. Since the intrablock coupling $\underline{H}(v:I_\nu)$ is stronger than the interblock coupling $\underline{H}(v:I_\nu, J_\nu)$, when the off-diagonal elements of $\underline{H}(v:I_\nu)$ become negligibly small, the matrix elements of $\underline{H}(v:I_\nu, J_\nu)$ can certainly be ignored. By comparing (3) and (7) with (16) and (21), the matrix element $H(v:I_\nu)_{ij}$ can be interpreted as the effective exchange coupling $\mathcal{J}_{\text{eff}}(v:I_\nu)_{ij}$ between two block spins, the configurations of which are represented by $|\Phi(v:I_\nu)_i\rangle$ and $|\Phi(v:I_\nu)_j\rangle$. Consequently, the fixed point corresponds to the condition that all block spins are decoupled.

III. THE MODEL

The most time-consuming part of the calculation is the matrix elements $\tilde{H}(v:I_\nu, J_\nu)_{ijkl}$. After many tests with various sizes of blocks, the most informative system which can be studied with a reasonably large amount of computer time is shown in Fig. 1. There are 18 identical cubes arranged in a simple-cubic lattice structure. The volume of each cube is a^3 , and the lattice constant of the background simple-cubic lattice is $a+d$. In each cube there are three randomly located spins of $\frac{1}{2}$. Any two spins \mathbf{S}_i and \mathbf{S}_j in the sample are separated by $r_{ij} \geq 0.3$, and interact with each other via the RKKY interaction

$$\mathcal{J}_{0,ij} = -\mathcal{J}_0 r_{ij}^{-3} \cos(2k_f r_{ij}). \quad (28)$$

We have set $k_f=5$ which is a reasonable value for non-magnetic host materials of dilute magnetic alloys, and $\mathcal{J}_0=1.1918$ which gives $\mathcal{J}_{0,ij}=-1$ at $r_{ij}=1$.

We first construct the set of configurations $\{|\Phi(0:I_0)\rangle; i=1, 2, \dots, 8\}$ for each cube with three spins, and then

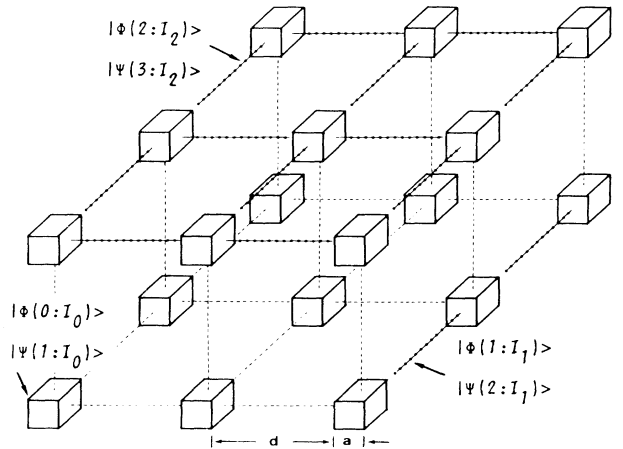


FIG. 1. A schematic description of the renormalization procedure.

derive the set of eigenstates $\{|\Psi(1:I_0)_i\rangle; i=1, 2, \dots, 8\}$. The three lowest-eigenenergies states $i=1, 2,$ and 3 are retained, and every three cubes are combined to form a block. One such block is shown in Fig. 1 as three cubes connected by a dotted line. The next step is to construct the set of configurations $\{|\Phi(1:I_1)_i\rangle; i=1, 2, \dots, 27\}$, from which we obtain the eigenstates $\{|\Psi(2:I_1)_i\rangle; i=1, 2, \dots, 27\}$. Again, we keep only the three lowest eigenenergies, states $i=1, 2,$ and 3 . Now, the six blocks are grouped into two blocks of equal size, and one of them is demonstrated in Fig. 1 as the nine cubes connected by dotted lines. We repeat the calculation by first constructing the sets of configurations $\{|\Phi(2:I_2)_i\rangle; i=1, 2, \dots, 27\}$ and then deriving the sets of eigenstates $\{|\Psi(3:I_2)_i\rangle; i=1, 2, \dots, 27\}$ for $I_2=1$ and 2 . For the last renormalization, we take eight eigenstates with $i=1, 2, \dots, 8$ from each set to build up 64 configurations $\{|\Phi(3:I_3)_i\rangle; i=1, 2, \dots, 64\}$. So at the end we have 64 eigenstates $\{|\Psi(F:I_3)_i\rangle; i=1, 2, \dots, 64\}$ of the entire system of 54 spins.

We set the external magnetic field $B=10^{-10}$ and the cube size $a=1$ to study two cases $d=0$ and 1 . The results are configurationally averaged over five samples.

As we mentioned in the preceding section, the matrix elements $H(v:I_v)_{ij}$ generalized from (21) play the role of effective coupling between block spins. We define a distribution $P(v:\mathcal{J}_{\text{eff}})$ of the effective exchange strength \mathcal{J}_{eff} as

$$P(v:\mathcal{J}_{\text{eff}}) = \frac{1}{2\Delta} \sum_{I_v} \sum_{i,j} \Theta(\mathcal{J}_{\text{eff}} + \Delta - H(v:I_v)_{ij}) \times \Theta(H(v:I_v)_{ij} - \mathcal{J}_{\text{eff}} + \Delta), \quad (29)$$

where $\Theta(x)$ is the Heaviside function. The results are shown in Fig. 2 for $d=0$ and in Fig. 3 for $d=1$. In each figure, the three histograms have the same scale for \mathcal{J}_{eff} . The number within parentheses at the top of each histogram indicates the true height of the peak. The peaks are truncated, and the numbers at the top mark the heights of the remaining parts which are plotted. It is clear from the two sequences of $P(v:\mathcal{J}_{\text{eff}})$ in Figs. 2 and 3 that our calculations converge very rapidly.

IV. PRELIMINARY INFORMATION

In our model the localization of eigenstates can be controlled by varying the distance d between cubes in Fig. 1. For given value of d , after deriving the eigenstates of the entire system $\{|\Psi(F:I_3)_i\rangle; i=1, 2, \dots, 64\}$, we can calculate the *local density* $\rho(i:I_v, \alpha)$ of $|\Psi(F:I_3)_i\rangle$

$$\rho(i:I_v, \alpha) = |\langle \Phi(v:I_v)_\alpha | \Psi(F:I_3)_i \rangle|^2 \quad (30)$$

with respect to the configuration space $\{|\Phi(v:I_v)_\alpha\rangle; \text{all } I_v, \alpha\}$. We define the *density-density correlation function* $\rho(v)_{ij}$ of the two eigenstates $|\Psi(F:I_3)_i\rangle$ and $|\Psi(F:I_3)_j\rangle$ as

$$\rho(v)_{ij} = \sum_{I_v} \sum_{\alpha} \rho(i:I_v, \alpha) \rho(j:I_v, \alpha), \quad i, j = 1, 2, \dots, 64.$$

(31)

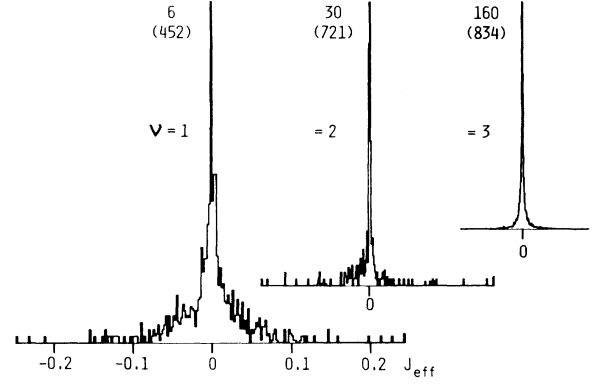


FIG. 2. Distribution $P(v:\mathcal{J}_{\text{eff}})$ of effective exchange \mathcal{J}_{eff} at different renormalization stage ν for the case $d=0$.

When $i=j, \rho(v)_{ii}$ is simply the inverse participation ratio of the state $|\Psi(F:I_3)_i\rangle$ with respect to the configuration space $\{|\Phi(v:I_v)_\alpha\rangle; \text{all } I_v, \alpha\}$.

If $\rho(v)_{ij}$ is large, then the two states $|\Psi(F:I_3)_i\rangle$ and $|\Psi(F:I_3)_j\rangle$ overlap very much in the configuration space $\{|\Phi(v:I_v)_\alpha\rangle; \text{all } I_v, \alpha\}$. Otherwise, the two states $|\Psi(F:I_3)_i\rangle$ and $|\Psi(F:I_3)_j\rangle$ are localized in different parts of the configuration space $\{|\Phi(v:I_v)_\alpha\rangle; \text{all } I_v, \alpha\}$. Since I_v labels the blocks which are separated in real space, $\rho(v)_{ij}$ also provides the information regarding the correlation of $|\Psi(F:I_3)_i\rangle$ and $|\Psi(F:I_3)_j\rangle$ in real space. In fact, for $\nu=0$ $\rho(0)_{ij}$ is indeed the density-density correlation function in real space.

The number of terms to be summed over in (31) increases tremendously fast from 8^2 for $\nu=3$, to 3^6 for $\nu=2$, to 3^{18} for $\nu=1$, and to 8^{18} for $\nu=0$. Figure 4 shows the results for $d=0$. For given point in the ij plane, the value of $\rho(v)_{ij}$ is indicated by the length of a vertical bar. Since we are interested in the values of $\rho(v)_{ij}$ relative to each other, for fixed ν the maximum value of $\rho(v)_{ij}$ is normalized to 1 and serves as the vertical scale. For both $\nu=3$ and $\nu=2$, the off-diagonal values $\rho(v)_{ij}$ are much less than the diagonal values $\rho(v)_{ii}$, especially, for the

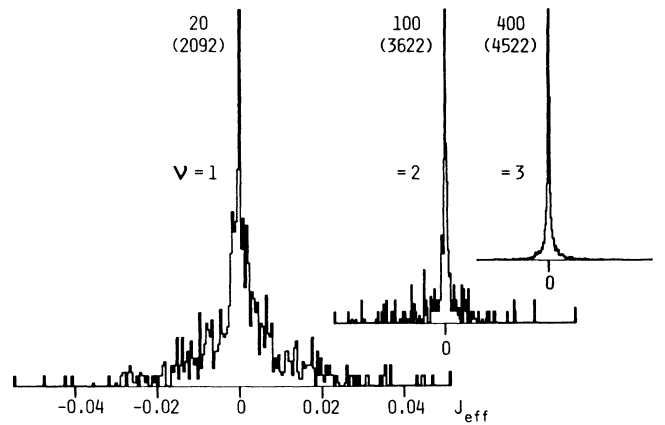


FIG. 3. Same as Fig. 2 for $d=1$.

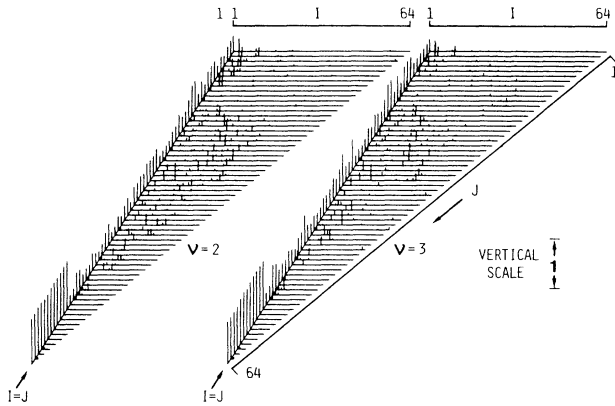


FIG. 4. Density-density correlation function $\rho^{(\nu)}_{ij}$ for the case $d=0$.

low-lying eigenstates corresponding to small values of i and j . Similar results for $d=1$ are shown in Fig. 5. In this case the cubes in Fig. 1 are fairly separated in space, and the eigenstates are expected to localize in individual cubes. However, for $\nu=2$ (or 3) each block contains three (or nine) cubes. At these levels ($\nu=2$ and 3) of calculation, the off-diagonal correlation function $\rho^{(\nu)}_{ij}$ is not negligibly small even if the states $|\Psi(F:I_3)_i\rangle$ and $|\Psi(F:I_3)_j\rangle$ are localized in two different cubes, provided that these two cubes are in the same block.

To calculate each term $\rho(i:I_\nu, \alpha)\rho(j:I_\nu, \alpha)$ in (31), one has to repeatedly use transformations of the types in Eqs. (18) and (23). It will take an unrealistic amount of computer time to calculate $\rho(1)_{ij}$ and $\rho(0)_{ij}$ with an ordinary computer. Nevertheless, the two plots for $\nu=2$ and $\nu=3$ in both Figs. 4 and 5 are almost the same, suggesting that the characteristic features of these figures remain unchanged even for $\nu=1$ and $\nu=0$. Consequently, it is not unreasonable to assume that the low-lying eigenstates $|\Psi(F:I_3)_i\rangle$ localize in different regions of the system and are fairly separated spatially. This conclusion will be supported by the following study on the distribution of internal fields.

The distribution of internal fields \mathbf{h}_i at various spins is

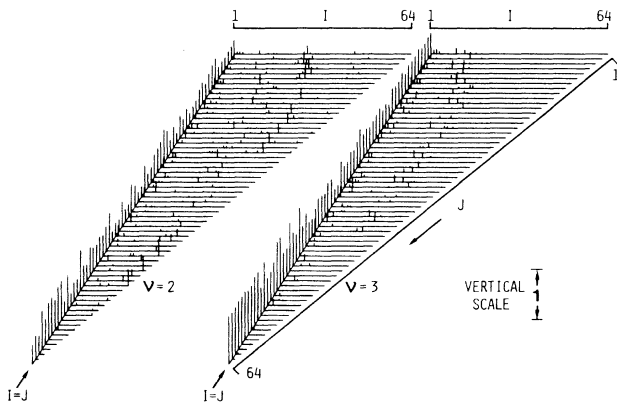


FIG. 5. Same as Fig. 4 for $d=1$.

an essential problem of spin glasses. There has been extensive investigation, mostly with numerical methods on the internal fields in classical Heisenberg spin glasses.³⁰⁻³⁷ Results derived by all authors agree that the distribution $P(|\mathbf{h}|)$ has zero value at $\mathbf{h}=0$. On the other hand, the distribution $P(h_z)$ of the z component of the internal field has a broad maximum at $h_z=0$.³¹

Knowing all eigenstates, we can calculate the internal field at i th spin

$$\mathbf{h}_i = \sum_j \mathcal{J}_{0,ij} \langle \mathbf{S}_j \rangle + \mathbf{B}, \quad (32)$$

where $\langle \dots \rangle$ is the thermal average. However, the computation of $\langle S_j^x \rangle$ and $\langle S_j^y \rangle$ is extremely tedious and too time consuming to be carried out at the moment. Here, we present only the results for the z component of internal field $h_{i,z}$. Similar to (29), we define the normalized distribution of the z component of internal field as

$$P(h_z) = \frac{1}{N} \frac{1}{2\Delta} \sum_i \Theta(h_z + \Delta - h_{i,z}) \Theta(h_{i,z} - h_z + \Delta), \quad (33)$$

where $N=54$ is the number of spins. The external field $\mathbf{B} = B\hat{z}$ in our calculation is extremely small $B = 10^{-10}$.

The temperature is normalized with respect to \mathcal{J}_0 as $k_B T / \mathcal{J}_0$. Figure 6 shows the distribution $P(h_z)$ for the case $d=0$ with four temperatures $k_B T = 10^{-6}$, 10^{-3} , 10^{-2} , and $10^{-1.5}$. At the lowest temperature 10^{-6} , only the ground state is occupied. However, within the thermal energy $k_B T = 10^{-1.5}$, there are already seven low-lying excited states. All four histograms have the same scale for h_z and for $P(h_z)$. We see in every histogram there is a sharp peak at $h_z=0$. As the temperature increases and more excited states contribute to $P(h_z)$, there is only a very gradual narrowing of the whole $P(h_z)$ curve. This result strongly suggests that these low-lying eigenstates contribute almost equally to the distribution $P(h_z)$. One possibility is that these low-lying eigenstates are spatially separated and localized on different clusters of spins. Such clusters are random in nature, and therefore the magnetic property of one cluster eigenstate is similar to those of the other cluster eigenstates.

Figure 7 shows the similar behavior of the distribution

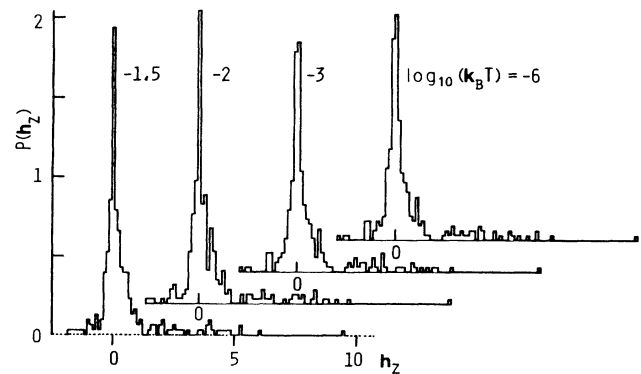


FIG. 6. Distribution $P(h_z)$ of the z component of internal field h_z for the case $d=0$.

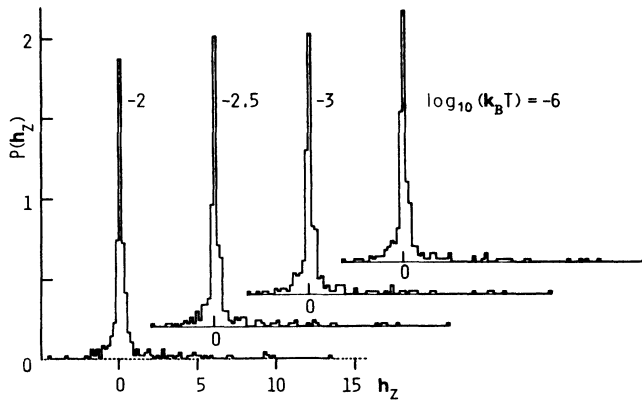


FIG. 7. Same as Fig. 6 for $d = 1$.

$P(h_z)$ for the case $d = 1$. There are about nine excited states with energies less than the thermal energy $k_B T = 10^{-2}$, but only the ground state contributes to $P(h_z)$ at $k_B T = 10^{-6}$. In this case, the cubes in Fig. 1 are fairly separated. Consequently, most likely the low-lying eigenstates are spatially disconnected. Such a physical picture is in favor of our conjecture presented in the preceding paragraph.

V. SPIN-GLASS BEHAVIOR

As we pointed out in the preceding section, at the moment there is a technical difficulty to compute $\langle S_i^x \rangle$ and $\langle S_i^y \rangle$. Hence, we will calculate instead the Edwards-Anderson spin-glass order parameter

$$Q(T) = \frac{1}{N} \sum_i \langle S_i^z \rangle^2. \quad (34)$$

The dc magnetic susceptibility $\chi(T)$ and the magnetic specific heat $C(T)$ are also calculated with the standard formula.

Figure 8 shows the results for the case $d = 0$. The scale

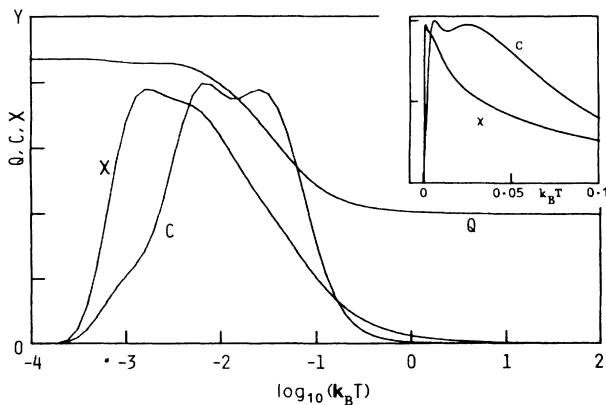


FIG. 8. Spin-glass order parameter Q ($Y = 0.025$), dc magnetic susceptibility χ ($Y = 1$), and magnetic specific heat C ($Y = 0.025$) for the case $d = 0$. The inset is for linear temperature scale.

for the vertical axis is $y = 0.025$ for Q , $y = 0.025$ for C , and $y = 1$ for χ . At low temperature the order parameter $Q(T)$ is finite and stays almost constant in the region $k_B T \leq 10^{-2}$. From the computed eigenenergies, we found that in all five samples the energy difference between the ground state and the first excited state is about $10^{-3.5}$. From Fig. 8, we see that in the temperature region $10^{-3} \leq k_B T \leq 10^{-2}$, $\chi(T)$ is also almost constant. We mentioned earlier that in this temperature region there are about seven low-lying excited states. Here we see again almost equal contribution to the order parameter $Q(T)$ and the susceptibility $\chi(T)$ from each low-lying eigenstate. This finding is consistent with our conjecture that the low-lying eigenstates are localized in spatially separated regions.

In the temperature region where the magnetic specific heat $C(T)$ has two broad peaks, both the order parameter $Q(T)$ and the susceptibility $\chi(T)$ decrease as temperature increases. Whilst $\chi(T)$ drops to zero at high temperature, $Q(T)$ levels off to a constant value. This level off is due to the truncation of high-lying eigenstates in our renormalization procedure. If all eigenstates were kept, $Q(T)$ should vanish at high temperature. When $Q(T)$ begins to level off, the magnetic specific heat $C(T)$ also levels off to zero. The maximum excitation energy in each of our five samples is around $k_B T = 0.1$. Consequently, our results are not reliable for temperatures higher than $k_B T \approx 10^{-1.5}$. Similar behaviors of $Q(T)$, $\chi(T)$, and $C(T)$ are shown in Fig. 9 for the case $d = 1$. The order parameter, the dc magnetic susceptibility, and the magnetic specific heat discussed above suggest that the spins are frozen in the ground state and the low-lying excited states.

VI. REMARKS

Our renormalization procedure and our computation scheme are very general and are applicable to any type of quantum-spin system with any type of exchange interaction. We should compute important correlation functions, vary the number of spins and repeat the calculation, increase the number of samples for a better configuration

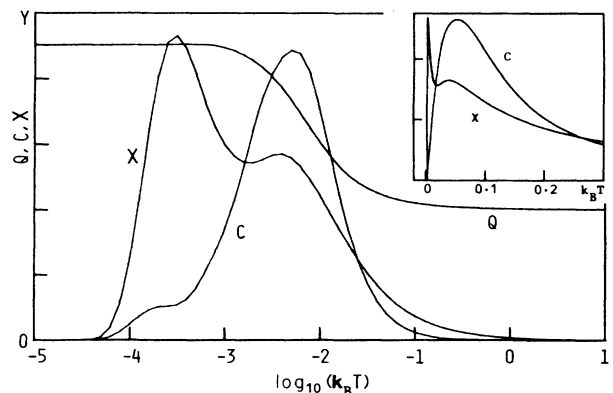


FIG. 9. Same as Fig. 8 for $d = 1$. The value of Y is 0.02 for Q , 0.03 for C , and 3 for χ .

average, and perform a finite-size scaling. Unfortunately, at the moment these works are restricted by the available computation facility. It is important to study the Parisi order function.³⁸ However, it is well known that in a finite system the Parisi order function is just a set of δ peaks.

We are aware of the unrealistic geometric structure of the model system for $d=1$. In this case all low-lying eigenstates are well localized in individual cubes. However, we simply use such well-determined properties to confirm that in the more realistic model system for $d=0$, the low-lying eigenstates are fairly localized around spatially separated clusters of spins.

The insets in Figs. 8 and 9 show the dc magnetic susceptibility $\chi(T)$ and the magnetic specific heat $C(T)$ as functions of temperature. The behavior of $\chi(T)$ is con-

sistent with the Monte Carlo calculations of Walstedt and Walker¹⁶ and Chakrabarti and Dasgupta¹⁹ with classical Heisenberg spins. On the other hand, the behavior of the order parameter $Q(T)$ in our quantum spin system suggests a continuous freezing of magnetic moment with decreasing temperature. Therefore, it is important to extend the present work to calculate the ac magnetic susceptibility. It will be very interesting to compare the calculated ac susceptibility to the puzzling experimental observations on different spin-glass materials.³⁹⁻⁴²

ACKNOWLEDGMENT

The work was financially supported by the Swedish Natural Science Research Council under Grant No. F-FU 3996-136.

-
- ¹For recent reviews, see R. Rammal and J. Souletie, in *Magnetism of Metals and Alloys*, edited by M. Cyrot (North-Holland, New York, 1982); *Heidelberg Colloquium on Spin-Glasses*, edited by J. L. van Hemmen and I. Morgenstern (Springer-Verlag, Berlin, 1983); K. H. Fischer, *Phys. Status Solidi B* **116**, 357 (1983); **130**, 13 (1985); D. Chowdhury and A. Mookerjee, *Phys. Rep.* **114**, 1 (1984); K. Binder and A. P. Young (unpublished).
- ²D. Sherrington and S. Kirkpatrick, *Phys. Rev. Lett.* **35**, 1792 (1975).
- ³W. L. McMillan, *Phys. Rev. B* **30**, 479 (1984); A. J. Bray and M. A. Moore, *J. Phys. C* **17**, L463; **17**, L613 (1985); *Phys. Rev. B* **31**, 631 (1985); R. N. Bhatt and A. P. Young, *Phys. Rev. Lett.* **54**, 924 (1985); A. T. Ogielski and I. Morgenstern, *ibid.* **54**, 928 (1985).
- ⁴J. R. Banavar and M. Cieplak, *Phys. Rev. Lett.* **48**, 832 (1982); W. L. McMillan, *Phys. Rev. B* **31**, 342 (1985).
- ⁵S. F. Edwards and P. W. Anderson, *J. Phys. F* **5**, 965 (1975).
- ⁶K. H. Fischer, *Phys. Rev. Lett.* **34**, 1438 (1975).
- ⁷R. A. Klemm, *J. Phys. C* **12**, L735 (1979).
- ⁸A. J. Bray and M. A. Moore, *J. Phys. C* **13**, L655 (1980).
- ⁹D. J. Thouless, P. W. Anderson, and R. G. Palmer, *Philos. Mag.* **35**, 593 (1977).
- ¹⁰H.-J. Sommers and K. D. Usadel, *Z. Phys. B* **47**, 63 (1982).
- ¹¹B. W. Morris, *Phys. Lett.* **110A**, 415 (1985).
- ¹²A. Theumann, *Phys. Rev. B* **33**, 559 (1986).
- ¹³H. Nishimori, Y. Taguchi, and T. Oguchi, *J. Phys. Soc. Jpn.* **55**, 656 (1986).
- ¹⁴W. Y. Ching and D. L. Huber, *J. Phys. F* **8**, L63 (1978).
- ¹⁵F. Fernandez and T. S. J. Streit, *Phys. Rev. B* **25**, 6910 (1982).
- ¹⁶R. E. Walstedt and L. R. Walker, *Phys. Rev. Lett.* **47**, 1624 (1981); *J. Appl. Phys.* **53**, 7985 (1982).
- ¹⁷R. E. Walstedt, *Physica* **109&110B+C**, 1924 (1982).
- ¹⁸L. R. Walker and R. E. Walstedt, *J. Magn. Magn. Mater.* **31-34**, 1289 (1983).
- ¹⁹A. Chakrabarti and C. Dasgupta, *Phys. Rev. Lett.* **56**, 1404 (1986).
- ²⁰A. J. Bray, M. A. Moore, and A. P. Young, *Phys. Rev. Lett.* **56**, 2641 (1986).
- ²¹S. D. Drell, M. Weinstein, and S. Yankielowicz, *Phys. Rev. D* **16**, 1769 (1977). For general descriptions of its use in spin systems, see Bambi Hu, *Phys. Rep.* **91**, 233 (1982); P. Pfeuty, R. Jullien, and K. A. Penson, in *Real-Space Renormalization*, edited by T. W. Burkhardt and J. M. J. van Leeuwen (Springer-Verlag, Berlin, 1982), p. 119.
- ²²R. Jullien, J. N. Fields, and S. Doniach, *Phys. Rev. B* **16**, 4889 (1977).
- ²³R. Jullien, P. Pfeuty, J. N. Fields, and S. Doniach, *Phys. Rev. B* **18**, 3568 (1978); R. Jullien and P. Pfeuty, *ibid.* **19**, 4646 (1979); K. A. Penson, R. Jullien, and P. Pfeuty, *ibid.* **19**, 4653 (1979); **22**, 380 (1980); **25**, 1837 (1982); J. E. Hirsch, *ibid.* **20**, 3907 (1979).
- ²⁴J. E. Hirsch and G. F. Mazenko, *Phys. Rev. B* **19**, 2656 (1979).
- ²⁵S. K. Sarker, *Phys. Rev. B* **30**, 2752 (1984).
- ²⁶S. T. Chui and J. W. Bray, *Phys. Rev. B* **18**, 2426 (1978); J. W. Bray and S. T. Chui, *ibid.* **19**, 4876 (1979).
- ²⁷J. E. Hirsch, *Phys. Rev. B* **22**, 5355 (1980); J. E. Hirsch and J. V. Jose, *ibid.* **22**, 5339 (1980); *J. Phys. C* **13**, L53 (1980).
- ²⁸J. N. Fields, *Phys. Rev. B* **19**, 2637 (1979).
- ²⁹J. M. Rabin, *Phys. Rev. B* **21**, 2027 (1980); **22**, 2420 (1980).
- ³⁰K. Binder, *Z. Phys. B* **26**, 339 (1977).
- ³¹F. A. De Rozario, D. A. Smith, and C. H. J. Johnson, *Physica* **86-88B**, 861 (1977).
- ³²L. R. Walker and R. E. Walstedt, *Phys. Rev. Lett.* **38**, 514 (1977).
- ³³R. G. Palmer and C. M. Pond, *J. Phys. F* **9**, 1451 (1979).
- ³⁴L. R. Walker and R. E. Walstedt, *Phys. Rev. B* **22**, 3816 (1980).
- ³⁵A. J. Bray and M. A. Moore, *J. Phys. C* **14**, 2629 (1981).
- ³⁶T. A. Kaplan and N. d'Ambrumenil, *J. Phys. C* **15**, 3769 (1982).
- ³⁷G. S. Grest and C. M. Soukoulis, *Phys. Rev. B* **28**, 2886 (1983).
- ³⁸G. Parisi, *Phys. Rev. Lett.* **43**, 1754 (1979); **50**, 1946 (1983).
- ³⁹H. von Lohneysen, J. L. Tholence, and R. Tournier, *J. Phys. (Paris) Colloq.* **39**, C6-922 (1978).
- ⁴⁰H. Maletta, W. Felsch, and J. L. Tholence, *J. Magn. Magn. Mater.* **9**, 41 (1978); H. Maletta and W. Felsch, *J. Phys. (Paris) Colloq.* **39**, C6-931 (1978).
- ⁴¹E. D. Dahlberg, M. Hardiman, and J. Souletie, *J. Phys. (Paris) Colloq.* **39**, C6-389 (1978); E. D. Dahlberg, M. Hardiman, R. Orbach, and J. Souletie, *Phys. Rev. Lett.* **42**, 401 (1979).
- ⁴²D. Korn, D. Schilling, and G. Zibold, *J. Phys. (Paris) Colloq.* **39**, C6-899 (1978); G. Zibold and D. Korn, *J. Magn. Magn. Mater.* **15-18**, 143 (1980).